NASA Technical Memorandum 89913
AIAA-87-9226

Fluoride Salts and Container Materials for Thermal Energy Storage Applications in the Temperature Range 973 to 1400 K

Ajay K. Misra and J. Daniel Whittenberger
Lewis Research Center
Cleveland, Ohio

Prepared for the
22nd Intersociety Energy Conversion Engineering Conference
cosponsored by the AIAA, ANS, ASME, SAE, IEEE, ACS, and AIChE
Philadelphia, Pennsylvania, August 10-14, 1987

NASA

FLUORIDE SALTS AND CONTAINER MATERIALS FOR THERMAL ENERGY STORAGE APPLICATIONS IN THE TEMPERATURE RANGE 973 TO 1400 K

Ajay K. Misra* and J. Daniel Whittenberger
National Aeronautics and Space Administration
Lewis Research Center
Cleveland, Ohio 44135

SUMMARY

Multicomponent fluoride salt mixtures were characterized for use as latent heat of fusion heat storage materials in advanced solar dynamic space power systems with operating temperatures in the range of 973 to 1400 K. The melting points and eutectic compositions for many systems with published phase diagrams were verified, and several new eutectic compositions were identified. Additionally the heats of fusion of several binary and ternary eutectics and congruently melting intermediate compounds were measured by differential scanning calorimetry. The extent of corrosion of various metals by fluoride melts was estimated from thermodynamic considerations, and equilibrium conditions inside a containment vessel were calculated as functions of the initial moisture content of the salt and free volume above the molten salt. Preliminary experimental data on the corrosion of commercial, high-temperature alloys in $LiF-19.5CaF_2$ and $NaF-27CaF_2-36MgF_2$ melts are presented and compared to the thermodynamic predictions.

INTRODUCTION

Latent heat of fusion phase change materials are being considered for heat storage in advanced solar dynamic space power systems. In order to keep the total weight of the space power system to a minimum, the phase change material must have a high heat of fusion per unit mass. It is anticipated that heats of fusion greater than 0.4 kJ/g would be needed. Also to minimize the weight of the container material, use of a phase change material with a high heat of fusion per unit melt volume would be desirable. Finally as current efforts are being focussed on Brayton and Stirling cycle heat engines with operating temperatures in the range of 973 to 1400 K (ref. 1), the melting point of the phase change material must lie within this temperature range.

There are only a few inorganic fluoride salts, i.e., NaF, KF, and LiF, which meet the melting point and heat of fusion requirements. These fluorides can be used only if the operating temperature of the heat engine is compatible with their melting points; this condition puts severe restrictions on the choice of the operating temperature for the heat engine. However, this limitation can be removed if fluoride based eutectic mixtures and/or congruently melting intermediate compounds are considered. Unfortunately little, other than compositions and melting points, is known about such systems, and in many cases the published phase diagrams are of questionable accuracy because the data determined by different authors are often in poor agreement. In addition

---

*Department of Metallurgy and Materials Science, Case Western Reserve University, Cleveland, Ohio 44106 and NASA Lewis Resident Research Associate.

to the need for reliable thermochemical and thermophysical data, compatibility of the multicomponent fluoride salt systems with possible materials of construction must be studied to select a suitable containment vessel material.

This report describes the results of our studies on (1) characterization of multicomponent fluoride salt mixtures, and (2) corrosion of commercial, high-temperature alloys in several fluoride melts. The melting points and eutectic compositions for many systems with published phase diagrams were experimentally verified, and new eutectic compositions with melting points between 973 and 1400 K were identified. The heats of fusion of several binary and ternary eutectics and congruently melting intermediate compounds were experimentally measured by differential scanning calorimetry. Additionally thermodynamic calculations have been made to determine the probable extent of corrosion of metals in fluoride melts with and without the moisture in the system. Preliminary results on the corrosion of commercial, high-temperature alloys in fluoride melts will also be presented.

THERMAL ANALYSIS AND HEAT OF FUSION MEASUREMENTS

Experimental Procedure

Melting points and heats of fusion of salt mixtures were measured in a Perkins Elmer DTA 1700 instrument. Heat of fusion measurements were made by utilizing the instrument in the differential scanning calorimetry (DSC) mode. A detailed discussion of the salt purification steps and exact experimental procedures are reported elsewhere (ref. 2).

Systems With Published Phase Diagrams

Table I gives a summary of heat of fusion and melting point measurements for eutectic compositions and congruently melting intermediate compounds for salt systems with known phase diagrams. This table also contains the melting points and heats of fusion of pure fluoride salts for comparison. With the exception of eutectic compositions in the LiF-MgF_2 and KF-MgF_2 systems and the congruently melting intermediate compound $NaMgF_3$ in NaF-MgF_2, there was close agreement (within 5 K) between the measured and published melting points. The melting temperature for the intermediate compound $NaMgF_3$ was found to be 8 K lower than that of Bergman et al. (ref. 7), and the melting point for KF-15MgF_2 was 12 K higher than the published data of DeVries and Roy (ref. 8).

There appears to be considerable uncertainty in the published LiF-MgF_2 phase diagram. Bergman and Dergunov (ref. 7) investigated this system and found a complete series of solid solutions between LiF and MgF_2 with a minimum melting point at about 33 mol % MgF_2. The phase diagram data of Counts et al. (ref. 9) show extensive solid solubility on each side of the phase diagram with an eutectic at 36 mol % MgF_2, although the existence of the eutectic was not conclusively established. Limited thermal analysis experiments by Roake (ref. 10) suggest the presence of an eutectic with a melting temperature of 997 K; unfortunately Roake's study was limited to only 15, 40, and 50 mol % MgF_2, and the exact eutectic composition was not determined. Because of poor agreement among the investigators of the LiF-MgF_2 system, we have conducted in-depth thermal analysis experiments for LiF-MgF_2 mixtures in the range of 0 to 50 mol % MgF_2. The thermal analysis data, shown in

table II, indicate an eutectic at about 30 mol % MgF_2 and with a melting temperature of 1001 K.

Among the salt systems with published phase diagrams, there are only a few salt mixtures with very high heat of fusion per unit mass: LiF-19.5CaF_2 at 0.82 kJ/g, NaF-60MgF_2 at 0.71 kJ/g, KF-69MgF_2 at 0.77 kJ/g and $KMgF_3$ at 0.71 kJ/g. As shown in table I, all the above salts are also likely to have high heat of fusion per unit liquid volume. Additionally LiF-20CeF_3 seems to be a suitable candidate if high heat of fusion per unit liquid volume is required, even though it has a relatively low heat of fusion per unit mass (0.5 kJ/g). This is due to the higher liquid density (~4.63 g/cm^3) for CeF_3 (ref. 6) as compared to the alkali fluoride melts (~1.8 and ~1.8 g/cm^3 for LiF and NaF melts respectively) (ref. 5).

Identification of New Eutectic Compositions

Since LiF has a very high heat of fusion per unit mass (1.08 kJ/g), it is anticipated that an eutectic between LiF and another compound would also have a reasonably high heat of fusion per unit mass provided there is no extensive solid solution between the two. The heat of fusion measurements (table I) show that the intermediate compounds $NaMgF_3$ and $KMgF_3$ have very high heat of fusion per unit mass (0.67 and 0.71 kJ/g, respectively); therefore, examination of mixtures of these intermediate compounds and LiF could reveal useful phase change salts. To identify possible eutectic compositions in these systems, the partial phase diagrams for the two quasi-binary systems have been determined by differential thermal analysis. As can be seen in figures 1 and 2 both LiF-$NaMgF_3$ and LiF-$KMgF_3$ have eutectics with extremely limited or no solid solubility within the composition ranges investigated.

MgF_2 also has a very high heat of fusion per unit mass and a high melting point; therefore it is of interest to identify potential MgF_2-base systems, particularly, for higher temperature (1300 to 1400 K) applications. The partial phase diagram for one MgF_2-base system, MgF_2-CeF_3, has been determined, and it has an eutectic at 1393 K with no solid solutions (fig. 3).

Table III lists the melting points and heats of fusion for the three newly identified eutectic compositions. The eutectic for the quasi-binary LiF-$KMgF_3$ system has a very high heat of fusion per unit mass (0.86 kJ/g) and thus would be attractive for space power applications. Even though it has a low heat of fusion per unit mass, the MgF_2-CeF_3 eutectic might be attractive on a volume basis.

Problem of Undercooling

Undercooling was observed in many systems, and table IV shows the extent for pure salts and mixtures. Because of considerable scatter in undercooling for different runs of the same sample, a range of values for the extent of undercooling is shown in table IV. The reported undercoolings are for very small sample sizes and high purity materials normally used in the thermal analysis experiments. Since small, high purity samples tend to undercool more than large, less pure materials, the degree of undercooling is expected to be lower in actual service conditions. Thus for many salt systems where the undercooling is 20 K or less, there might not be any practical problems. However when

the intermediate compound $NaMgF_3$ was formed, the undercooling was considerable (>30 K), and it could be a serious problem in actual service conditions if NaF-MgF_2-based systems are used.

THERMODYNAMIC CONSIDERATIONS FOR CORROSION OF METALS IN THERMAL ENERGY STORAGE SYSTEMS

A schematic of a thermal energy salt container is shown in figure 4. It has been partially filled and then sealed by welding in either an inert atmosphere or a vacuum. The salt-filled container is placed in a heat transfer fluid, which during the sunlit portion of each orbi (about 1 hr) provides the energy to melt the salt. The heat stored in the phase change material is then extracted by the same heat transfer fluid during the eclipse portion of each orbit (~1/2 hr), as the salt solidifies. Since the atmosphere above the salt is initially inert, the primary mode of attack is expected to be direct reaction of the metals with the salt melt. However, additional modes of degradation could be introduced if the salt contains impurities such as water. In the following, thermodynamic calculations are presented to define the equilibrium conditions for possible corrosion reactions. For a given set of conditions, the equilibrium state represents the maximum extent of corrosion; therefore it would play an important role in assessing the long-term life of a containment material.

Methodology of Calculations

The equilibrium calculations were performed between 1000 and 1300 K by utilizing the concept of "extent of reaction" (refs. 11 and 12) and for one mole of salt in the container. For temperatures below the melting points of the salts, the Gibbs standard free energy for liquid fluorides were computed by standard thermodynamic procedures (ref. 13) utilizing the heat of fusion data at the melting point and the heat capacity as a function of temperature for both the liquid and solid states. Wherever possible the thermodynamic data were taken from Barin and Knacke's compilations (ref. 3); however the thermodynamic properties for several liquid fluorides (i.e., CrF_2, CrF_3, NiF_2, FeF_2, and CoF_2) are not known and had to be estimated. While the main features of the calculations are given; the detailed descriptions are elsewhere (ref. 14).

Reaction of Fe, Ni, Co, Cr, and Al with Fluoride Melts in an Inert Atmosphere

In the absence of an oxidizing atmosphere, corrosion of a pure metal Me (Me = Fe, Ni, Co, Cr, or Al) in an alkali fluoride (MF, M = Li, Na, or K) melt would occur by the reaction

$$x\,Me(s) + y\,MF(l) = \underline{Me_xF_y(l)} + y\,\underline{M(l)} \qquad (1)$$

where the underlining denotes that the species are present at reduced activity. For Ni, Co, Fe, and Cr the relevant Me_xF_y compounds are NiF_2, CoF_2, FeF_2, CrF_2/CrF_3, respectively. Although the reaction of Al with MF would result in formation of AlF_3, the heat of mixing data for MF-AlF_3 melts (ref. 15) suggest the existence of complex species AlF_6^{3-} which is equivalent to the formation of

M_3AlF_6 by the reaction of MF and AlF_3. Therefore the reaction of Al with the MF melts can be written as

$$6\ MF(l) + Al(s) = M_3AlF_6(l) + 3\ M(l) \qquad (2)$$

The equilibrium content of Me_xF_y (for Ni, Co, Fe, Cr) and M_3AlF_6 in the melt determines the maximum extent of corrosion, and the purpose of thermodynamic calculations is to estimate these concentrations.

Figure 5 shows the calculated equilibrium concentrations of various metal fluorides in alkali fluoride melts at 1100 K for corrosion of the pure metals under an inert atmosphere where ideal solution behavior was assumed for the melt. In all three systems the tendency for metals to corrode increases in the order: Ni, Co, Fe, Cr, Al. The equilibrium concentration of M_3AlF_6 in the molten salts is so high that alloys containing significant amounts of Al are expected to suffer severe corrosion. Even though these calculations were performed for unit activity, the same conclusion would still hold when Al is present at a reduced activity. For example, taking the activity of Al in Ni_3Al (the strengthening phase in Ni-base superalloys) to be on the order of 10^{-5} (ref. 16), the equilibrium concentrations for Al in LiF and NaF melts at 1100 K would be 41 and 7360 mol ppm, respectively. Although these Al concentrations are lower than those for unit activity, they are sufficient to cause major corrosion of Al-containing alloys.

it is basing the corrosivity of the salt only on the formation of metal fluorides and says Ni, Fe and CO are safe in NaF

From figure 5 it can be seen that LiF is the least corrosive salt while NaF and KF are about equal in their attack. The equilibrium concentration of Ni, Co, Fe, and Cr fluorides in a LiF melt are quite small (<<1 mol ppm); thus alloys containing these elements are expected to be corrosion resistant. Ni, Fe, and Co are also anticipated to be free from damage in NaF and KF melts; on the other hand, alloys containing Cr might be corroded by these two melts because of higher solubility of Cr in the form of CrF_2 (for example, 12 mol ppm for CrF_2 as compared to approximately 0.1 mol ppm for FeF_2). It appears that the formation of CrF_3 is not important for corrosion of Cr due to its much lower solubility (about 2 orders of magnitude lower than that as CrF_2).

The equilibrium concentrations of different metal fluorides in figure 5 were calculated under the assumption of ideal solution behavior in the melt, that is, the activity coefficient (γ) of Me_xF_y in the melt was assumed to be unity. Although activity coefficients for Me_xF_y in alkali fluoride melts have not been measured; in systems for which phase diagrams are available, they can be estimated from an analysis of the phase diagrams (ref. 17) and are shown in table V. As the activity coefficients are considerably less than unity, a strong negative interaction seems to exist in all the $MF\text{-}Me_xF_y$ type melts. In view of the estimates in table V, the activity coefficient of Me_xF_y for systems without phase diagrams (all $LiF\text{-}Me_xF_y$ systems and $NaF\text{-}CrF_2$) will be assumed to be 0.001 in the following equilibrium calculations.

The effect of the nonideality and temperature on the equilibrium concentration of Me_xF_y in a LiF melt is shown in figure 6. Compared to the ideal solution behavior (fig. 5), there is an order of magnitude increase in the concentration of Me_xF_y at 1100 K; even with such an increase, the equilibrium concentration of NiF_2 is still less than 0.01 mol ppm. Over the 1000 to 1200 K temperature range shown in this figure, the amounts of Me_xF_y in the molten salts would increase about one order of magnitude. It is anticipated

that the corrosion of Fe and Ni would be minimal because of the low concentrations of FeF_2 and NiF_2; on the other hand, the equilibrium concentration of CrF_2 at 1200 K (14 mol ppm) is probably sufficient to cause some attack of Cr containing alloys at this temperature.

Figure 7 shows the equilibrium Me_xF_y concentrations between 1100 and 1300 K in a NaF melt utilizing the estimated activity coefficients for Me_xF_y. Since the equilibrium concentration of NiF_2 is very low, Ni is expected to be corrosion resistant. On the other hand, Fe will probably suffer from significant corrosion, particularly at higher temperatures, as the final concentrations of FeF_2 in a NaF melt at 1200 and 1300 K were estimated to be 25 and 73 mol ppm, respectively. Additionally the equilibrium concentrations of CrF_2 were computed to be 100 mol ppm for 1100 K and 900 mol ppm for 1300 K; thus Cr-containing alloys might not be suitable for NaF-containing melts.

Corrosion of a metal Me in MgF_2 or CaF_2 melt can be written as

$$x\ Me(s) + y\ AF_2(l) = \underline{Me_xF_y(l)} + \underline{y\ A(l)} \qquad (3)$$

where A represents either Ca or Mg. Calculation of the equilibrium concentration of NiF_2 and CrF_2 in a hypothetical MgF_2 melt at 1100 K with the assumption of ideal solution behavior in the melt yields 1.9×10^{-5} mol ppm for NiF_2 and 0.08 mol ppm for CrF_2. These values are three orders of magnitude lower than those determined for corrosion in a NaF melt at 1100 K (fig. 5). Due to the greater thermodynamic stability of CaF_2, the extent of corrosion in a CaF_2 melt should even be lower than that in the MgF_2.

Reaction of Refractory Metals Nb, Mo, W With Fluoride Melts Under an Inert Atmosphere

There are no known condensed Nb, Mo, or W fluorides between 1000 and 1400 K; instead gaseous refractory fluorides are the stable phases. Consequently, the reaction of a refractory metal Me (Me = Nb, Mo, or W) with an alkali fluoride MF can be written as

$$x\ Me(s) + y\ MF(l) = Me_xF_y(g) + y\ \underline{M(l)} \qquad (4)$$

Since a gas phase is involved in equation (4), for a closed system the extent of the reaction would be a function of the empty space available inside a container. Therefore all the calculations were performed as a function of a dimensionless variable L which is defined as the ratio of the container volume to the molar volume of the salt melt. Table VI shows the amount of gaseous refractory metal formed per mole of NaF. The extent of reaction is quite small ($<10^{-7}$ mol of metal consumed per mole of the salt) for all the refractory metals; therefore no significant corrosion of refractory metals in NaF is expected. While corrosion in KF will be very similar to that in NaF melts, due to the greater thermodynamic stability of LiF, refractory metals should be even less prone to attack in LiF than in NaF or KF.

Role of Moisture in Corrosion

Water is a common impurity in the halide salts, and it has proven difficult to remove from fluorides (ref. 18). Unfortunately, the reaction of alkali fluorides with moisture generates gaseous HF by

$$MF(l) + H_2O(g) = \underline{MOH(l)} + HF(g) \quad (5)$$

$$2\ MF(l) + H_2O(g) = \underline{M_2O(l)} + 2\ HF(g) \quad (6)$$

Part of the HF gas will then dissolve in the melt by the reaction

$$HF(g) = \underline{HF(l)} \quad (7)$$

The simultaneous equilibria and mass balance constraints for reactions (eqs. (5) to (7)) were used to determine the partial pressures of HF and H_2O (P_{HF} and P_{HO}) above the melt, the total pressure in the container (P_T), and mole fraction of dissolved HF in the melt ($X_{HF(M)}$) as functions of the initial moisture content in the salt and L ratios. Results of these calculations for NaF melts at 1100 K and an initial total pressure of 0.001 atm are shown in figures 8 and 9. The gas pressures generated inside the container are strongly dependent on the initial moisture content irrespective of the free volume. On the other hand L is only an important variable when moisture levels exceed 100 ppm. From figure 8(d) it is clear that pressures greater than 1 atm can be generated for high water contents and small volumes. WHile such pressures could lead to mechanical failure of the containment vessel, they would not be generated if the initial moisture levels are controlled to ~100 mol ppm or less.

In addition to pressurizing the containment vessel, the presence of moisture in the salt generates HF. Thus corrosion would take place both in the melt, as aided by the dissolved HF, and in the free volume via attack from gaseous water and hydrogen fluoride. Figure 9 illustrates that the concentration of dissolved HF for 100 mol ppm of initial moisture in the salt is on the order of 10^{-4} mol per mole of NaF. If dissolved HF reacts with the metal containment vessel, serious corrosion problems could be anticipated. Furthermore, generation of H_2 gas by the corrosion reaction

$$x\ Me + y\ HF = Me_xF_y + \frac{y}{2} H_2 \quad (8)$$

will increase the total pressure inside the container. Thermodynamic calculations for L equal to 1.1 and with the assumption that all the dissolved HF reacts to form H_2 gas demonstrate (fig. 10) that the total pressure inside the container will exceed 1 atm at a lower initial moisture content (~40 mol ppm) compared to the case where there is no reaction between dissolved HF and the container material (~250 mol ppm).

From the thermodynamic analysis it is clear that the moisture content in NaF-based salts should be reduced to low levels, probably 10 mol ppm or less, for prolonged container life. A similar conclusion can also be made LiF- and KF-based salt systems.

CORROSION EXPERIMENTS

As part of the work in support of an advanced solar dynamic power system, corrosion studies in potential fluoride energy storage salts are being undertaken. Because of the large body of fabrication, joining and mechanical and physical property information which will eventually be required to build a heat receiver/storage unit, this effort is basically being limited to commercially available, high temperature sheet alloys; although in view of forementioned thermodynamic factors, such alloys which generally contain Al and/or Cr for oxidation resistance are probably not the best choice.

In brief about 30 Co-, Fe-, Ni-base and refractory alloys (table VII) have been exposed to several eutectic salt mixtures ($LiF-19.5CaF_2$ which melts at 1039 K and $NaF-27CaF_2-36MgF_2$ which melts at 1178 K) at $T_M + 25$ K where T_M is the eutectic melting point. Each experiment involved a metallic specimen in contact with molten salt in a sealed, evacuated quartz capsule and/or open alumina crucible under an argon atmosphere for times ranging from 50 to 500 hr. Because residual water in the salt was deemed to be detrimental, the salts were heated under vacuum prior to sealing (SiO_2 capsule) or introduction of the argon (Al_2O_3 crucible) to drive off excess H_2O. Upon completion of the exposure, the alloy samples were examined for evidence of corrosion by metallographic techniques.

Typical photomicrographs illustrating the types of microstructural damage are presented in figure 11. The least noxious is a general attack consisting of small, isolated near surface pores (fig.11(a); however it is apparent that general attack can produce interconnected porosity which becomes infiltrated with salt and leads to the stripping away of layers of metal (fig. 11(b)). Intergranular corrosion, as shown in figure 11(c), is usually a more severe form of damage with deep penetration into the alloy. Lastly metals which are heavily corroded exhibit both general and intergranular effects (fig. 11(d)). In any case as the proposed life for the advanced solar dynamic system is 7 years or more, any signs of attack, either general or intergranular, would severely limit the usefulness of the alloy.

Because it was noted in other work (ref. 19) that the salts attacked the quartz capsules during the corrosion exposures, there was concern that the reactions among fluorides and SiO_2 biased the results. The data in figure 12, which compares the depth of corrosive attack for several alloys exposed to $NaF-27CaF_2-36MgF_2$ in quartz capsules and alumina crucibles, reveals that the behavior and ranking is similar for both experimental techniques. However the extent of internal penetration is much greater for the alloys sealed in quartz, and it is most likely due to the combined effects of H_2 and SiO_2 reacting with the fluorides to form SiO_2 compounds. Additionally evidence that the presence of quartz by itself does not greatly affect the degree of attack in $NaF-27CaF_2-36MgF_2$ is presented in table VIII. In this case there is generally no difference (for example 304, 347, and Hastelloy-X) or very little deviation (310, 316 mild steel, Hastelloy-N, Ni, and Ta) between the microstructural damage found in test samples after 100 hr exposures in the molten eutectic adulterated or not adulterated with SiO_2.

A listing of the depth of both general and intergranular corrosive attack for the tests conducted in alumina crucibles is given in table VIII. It should be noted that most of the $LiF-19.5CaF_2$ leaked out of the Al_2O_3 crucibles during the 500 hr heat treatments: however as the degree of corrosion for these tests

scales with the 100 hr results (no loss of salt observed), the long term data is probably valid. Since the alloying elements in the high-temperature materials do not vary in a systematic manner, it is difficult to make overall statements about behavior, and only one distinct trend was found. For Ni-base alloys immersed in the molten LiF-19.5CaF_2 eutectic, the extent of attack generally increased with Cr content (fig. 13). A similar dependency was not observed in the Cr containing Fe-base alloys where the depth of corrosion for such alloys, which have between 16 and 27 percent Cr, was about 40 and 150 μm after 100 and 500 hr heat treatments respectively. Additionally the Co-based materials were corroded by the LiF-19.5CaF_2 mixture with damage extending to ~100 μm after 500 hr of exposure. Based on the present results for the non-refractory materials, only pure Ni appears to have sufficient corrosion resistance for long term use with LiF-19.5CaF_2. The alloy Hastelloy B (consisting of Ni, Mo, and Fe) might also be suitable in this salt melt.

The data for specimens which had been subjected to NaF-27CaF_2-36MgF_2 at 1203 K (table VIII) fell into three groups:

(1) The pure metals Mo and W and the alloys Hastelloy B and Nb-1Zr appear to have undergone very little, if any, attack.

(2) The ferritic alloy 18 S/R, Hastelloy X, 800 and pure Ta exhibited damage zones of about 40 μm.

(3) All the remaining Co-, Fe-, and Ni-base alloys experienced ~10 μm deep corrosion.

In view of previous work with three other NaF-based eutectics (ref. 19), it is not clear why the Ni-base alloys Hastelloy X and 800 were more severely attacked than the other nickel-rich materials, or why pure Ni and Fe experienced some corrosion.

While the thermodynamic calculations (fig. 6) indicated that Cr-containing alloys should not be subject to attack in LiF-based melts, the data in table VIII and figure 13 show that this is not the case for the present experiments in LiF-19.5CaF_2. Most likely this behavior is a result of either the included moisture which was not removed by the vacuum anneal prior to the corrosion exposures or the moisture (~200 ppm) present in the argon gas; additionally it is possible that reactions between this eutectic and alumina crucibles yielded chemical species which tended to increase the corrosivity of the molten salt. Comparison of the data from the ternary NaF system (table VIII) with the thermodynamic predictions (fig. 7) reveals that they are basically in agreement. The refractory metals Nb, Mo, and W and the Ni-Mo alloy Hastelloy B were not harmed, while the alloys with Cr experienced some microstructural damage.

SUMMARY OF RESULTS

Multicomponent fluoride salt mixtures, suitable for use as latent heat of fusion heat storage materials in advanced solar dynamic space power systems with operating temperatures in the range of 973 to 1400 K, were characterized via thermodynamic calculations and measurements and corrosion experiments. Several new eutectic compositions were identified in LiF-NaF-MgF_2, LiF-KF-MgF_2, and MgF_2-CeF_3, and the melting points and eutectic compositions for many other

fluoride base systems with published phase diagrams (for example $LiF-19.5CaF_2$, $NaF-23MgF_2$, etc.) were experimentally verified. The heats of fusion and extent of undercooling for a number of binary and ternary eutectics and congruently melting intermediate compounds were established by differential scanning calorimetry and differential thermal analysis, and undercooling was found to be significant for systems which form $NaMgF_3$.

Thermodynamic calculations were undertaken to estimate the corrosivity of molten fluoride salts in the absence of water. Similar determinations in addition to an evaluation of the internal pressure were made for sealed, salt filled containment vessels as functions of the initial moisture content and free volume above the melt. Such analyses clearly indicate that all fluorides must be essentially free of all included H_2O (<10 mol ppm) to prevent attack of common alloys. The results of corrosion experiments involving a large number of commercial, high-temperature alloys in $LiF-19.5CaF_2$ at 1070 K and $NaF-27CaF_2-36MgF_2$ at 1203 K are given and compared to the thermodynamic predictions.

REFERENCES

1. Juhasz, A.J., Coles-Hamilton, C.E., and Lacy, D.E., "Impact of Thermal Energy Storage Properties on Solar Dynamic Power Conversion System Mass," NASA TM-89909, 1987. (to be presented at the 22nd IECEC).

2. Misra, A.K., "Fluoride Salts as Phase Change Materials for Thermal Energy Storage in the Temperature Range 1000°-1400° K," submitted for publication in the Journal of the Electrochemical Society.

3. Barin, I. and Knacke, O., Thermochemical Properties of Inorganic Substances, Springer-Verlag, New York, 1973.

4. Janz, G.J., Gardner, G.L., Krebs, U., and Tomkins, R.P.T., "Molten Salts: Volume 4, Part 1, Fluorides and Mixtures. Electrical Conductance, Density, Viscosity, and Surface Tension Data," Journal of Physical and Chemical Reference Data, Vol. 3, No. 1, 1974, pp. 1-115.

5. Janz, G.J., Allen, C.B., Bansal, N.P., Murphy, R.M., and Tomkins, R.P.T., Physical Properties Data Compilations Relevant to Energy Storage, II. Molten Salts: Data of Single and Multi-Component Salt Systems, National Bureau of Standards, Washington D.C., NSRDS-NBS-61-PT-2, 1979.

6. Kirschenbaum, A.D., Cahill, J.A., and Stokes, C.S., "The Density of Molten Metal Fluorides in the Range of 1600°-2500° K," Journal of Inorganic and Nuclear Chemistry, Vol. 15, Nos. 3/4, 1960, pp. 297-304.

7. Bergman, A.G. and Dergunov, E.P., "Fusion Diagram of the System $LiF-NaF-MgF_2$," Comptes Rendus de l'Academie des Sciences de l'URSS (Doklady Akademii Nauk SSSR), Vol. 31, 1941, pp. 755-756.

8. DeVries, R.C. and Roy, R., "Fluoride Models for Oxide Systems of Dielectric Interest. The Systems $KF-MgF_2$ and $AgF-ZnF_2$," Journal of the American Chemical Society, Vol. 75, No. 10, May 20, 1953, pp. 2479-2484.

9. Counts, W.E., Roy, R., and Osborn, E.F., "Fluoride Model Systems: II, The Binary Systems CaF_2-BeF_2, MgF_2-BeF_2, and LiF-MgF_2," Journal of the American Ceramic Society, Vol. 36, No. 1, Jan. 1953, pp. 12-17.

10. Roake, W.E., "The Systems CaF_2-LiF and CaF_2-LiF-MgF_2," Journal of the Electrochemical Society, Vol. 104, No. 11, Nov. 1957, pp. 661-662.

11. Lupis, C.H.P., Chemical Thermodynamics of Materials, North-Holland, New York, 1983.

12. Rao, Y.K., "The Analysis and Calculation of Equilibria in Complex Metallurgical Systems," Metallurgical Transactions B, Vol. 14, No. 12, Dec. 1983, pp. 701-710

13. Kubaschewski, O. and Alcock, C.B., Metallurgical Thermochemistry, Fifth Edition, Pergammon Press, New York, 1979.

14. Misra, A.K., "Thermodynamic Considerations for Corrosion of Metals in Thermal Energy Storage Systems Utilizing Fluorides as Phase Change Materials," submitted for publication in Corrosion Science.

15. Hong, K.C. and Kleppa, O.J., "Thermochemistry of the Liquid Mixtures of Aluminium Fluoride with Alkali Fluorides and with Zinc Fluoride," Journal of Physical Chemistry, Vol. 82, No. 2, Feb. 1978, pp. 176-182.

16. Hultgren, R., Selected Values of the Thermodynamic Properties of Binary Alloys, American Society for Metals, Metals Park, OH, 1973.

17. Lumsden, J., Thermodynamics of Molten Salt Mixtures, Academic Press, New York, 1966.

18. Laitinen, H.A., Ferguson, W.S., and Osteryoung, R.A., "Preparation of Pure Fused Lithium Chloride-Potassium Chloride Eutectic Solvent," Journal of the Electrochemical Society, Vol. 104, No. 8, Aug. 1957, pp. 516-520.

19. Whittenberger, J.D. and Misra, A.K., "Identification of Salt-Alloy Combinations for Thermal Energy Storage Applications in Advanced Solar Dynamic Space Power Systems," Solar Engineering 1987, D.Y. Goswami, K. Watanabe, and H.M. Healey, eds., ASME, New York, 1987, pp. 356-365.

TABLE I. - SUMMARY OF MELTING POINT AND HEAT OF FUSION MEASUREMENTS FOR FLUORIDES WITH PUBLISHED PHASE DIAGRAMS

Composition, mol %	Melting point, K	Heat of fusion per unit mass, kJ/g	Heat of fusion per unit volume of the melt, kJ/cm^3
LiF-30MgF_2	1001	0.52	[c]1.07
NaF-22CaF_2-13MgF_2	1027	.54	[c]1.17
LiF-20CeF_3	1029	.5	[b]1.58
LiF-19.5CaF_2	1042	.82	[b]1.7
KF-15CaF_2	1053	.44	[c]0.88
KF-15MgF_2	1063	.52	[c]1.03
NaF-20MgF_2-16KF	1077	.65	[c]1.31
NaF-32CaF_2	1083	.6	[b]1.4
NaF-23MgF_2	1103	.63	[c]1.3
LiF	1121	[a]1.08	[b]1.96
KF	1129	[a].486	[b]0.93
NaF-40MgF_2-20CaF_2	1187	.59	[c]1.33
CaF2-50MgF_2	1250	.54	[c]1.34
NaF-60MgF_2	1269	.71	[c]1.48
NaF	1268	[a].79	[b]1.54
KF-69MgF_2	1279	.77	[c]1.73
$NaMgF_3$	1295	.67	[c]1.48
KF-61CaF_2	1328	.45	[c]1.02
$KCaF_3$	1343	.46	[c]1.01
$KMgF_3$	1345	.71	[c]1.52
MgF_2	1536	[a].93	2.26[b]

[a]Obtained from Barin and Knacke's compilations (ref. 3).

[b]Liquid density extrapolated from published data (refs. 4 to 6).

[c]Liquid density estimated by assuming (1) ideal solution behavior and (2) the molar volume of each component at its melting point does not change with temperature.

TABLE II. - PARTIAL PHASE DIAGRAM DATA FOR THE LiF-MgF_2 SYSTEM

MgF_2 concentration, mol %	Solidus temperature, K	Liquidus temperature, K
5	1063	1103
10	1041	1088
15	1014	1063
20	1003	1043
25	[a]1002	1020
28	[a]1001	1001
30	[a]1002	1002
33	[a]1001	1003
35	[a]1002	1073
40	[a]1002	1143
50	[a]1002	1253

[a]Eutectic temperature.

TABLE III. - COMPOSITION, MELTING POINT, AND HEAT OF FUSION FOR NEW EUTECTIC FLUORIDE SALTS

Composition, mol %	Melting point, K	Heat of fusion per unit mass, kJ/g	Heat of fusion per unit volume of the melt, kJ/cm^3
LiF-19NaF-19MgF_2 (LiF-23$NaMgF_3$)	966	0.69	[a]1.39
LiF-13KF-13MgF_2 (LiF-15$KMgF_3$)	1022	.86	[a]1.67
MgF_2-40CeF_3	1393	.42	[a]1.5

[a]Liquid density estimated by assuming (1) ideal solution behavior and (2) the molar volume of each component at its melting point does not change with temperature.

TABLE IV. - EXTENT OF UNDERCOOLING FOR FLUORIDE SALTS

Composition, mol %	Degree of undercooling,[a] K
$LiF-30MgF_2$	0
$LiF-13KF-13MgF_2$	0
$NaF-22CaF_2-13MgF_2$	15 to 30
$LiF-20CeF_3$	0
$LiF-19.5CaF_2$	2 to 3
$KF-15CaF_2$	0
$KF-15MgF_2$	0
$NaF-20MgF_2-16KF$	20 to 30
$NaF-32CaF_2$	30 to 40
$NaF-23MgF_2$	60 to 80
LiF	0
KF	0
$NaF-40MgF_2-20CaF_2$	40 to 60
$CaF_2-50MgF_2$	3 to 20
$NaF-60MgF_2$	70 to 80
NaF	0
$KF-69MgF_2$	20
$NaMgF_3$	30 to 120
$KF-61CaF_2$	30 to 40
$KCaF_3$	20 to 30
$KMGF_3$	20 to 30
$MgF_2-40CeF_3$	7 to 20

[a]Range of values corresponds to the scatter in the data for different runs.

TABLE V. - ESTIMATED ACTIVITY COEFFICIENTS FOR DILUTE SOLUTIONS OF Me_xF_y IN MF - Me_xF_y MELTS

Melt system	Me_xF_y	Activity coefficient of Me_xF_y
$LiF-CrF_3$	CrF_3	0.001
$NaF-FeF_2$	FeF_2	.002
$NaF-NiF_2$	NiF_2	.01
$NaF-CrF_3$	CrF_3	.001

TABLE VI. - NUMBER OF MOLES OF GASEOUS REFRACTORY METAL FLUORIDE (n_g) FORMED PER MOLE OF SALT FOR REACTION OF THE METAL WITH A NaF MELT

Gaseous species	Temperature, K	$LOG(n_g)$, L = 1.1	$LOG(n_g)$, L = 2
NbF_5	1100	-7.5	-7.3
	1300	-6.4	-6.2
MoF_6	1100	-11.45	-11.3
	1300	-9.7	-9.6
WF_6	1100	-10.4	-10.3
	1300	-8.9	-8.75

TABLE VII. - SHEET ALLOYS PROPOSED FOR COMPATIBILITY STUDY

Alloy	Composition, at %												
	Fe	Cr	Ni	Co	Mn	Si	Mo	Nb	Ta	W	Al	C	Other
Cobalt base													
Haynes 188	1.7	28.2	24.1	38.2	0.7	1.6	----	----	----	5.2	---	0.4	0.05La
H25	3.4	24.1	10.7	52.5	1.7	2.2	----	----	----	1.1	---	.4	------
Nickel base													
Hastelloy-B	5.9	0.4	70.5	0.8	0.8	0.9	19.5	----	----	-----	1.	0.3	------
False N	.5	19.8	67.7	----	0.6	0.9	9.6	----	----	-----	0.7	.7	------
Hastelloy-N	5.1	8.3	72.9	----	.6	1.1	11.1	----	----	-----	.5	.3	0.24V
Hastelloy-S	0.9	19.6	66.1	----	.6	1.1	10.	----	----	.2	.7	1.0	------
Hastelloy-X	22.1	25.9	41.5	1.9	.6	1.2	5.2	----	----	.2	.9	.5	------
Inconel 600	9.7	18.9	69.9	----	.6	.2	----	----	----	-----	---	.5	.24Ti
Inconel 702	.5	19.4	73.	----	.1	.2	----	----	----	-----	5.9	.5	.5Ti
Inconel 718	19.5	22.9	48.9	----	.05	1.6	1.6	2.6	----	-----	1.3	.5	1.2Ti
Nimonic 75	.5	24.4	72.	----	.4	1.6	----	----	----	-----	.6	.05	------
Ni-200	----	----	99.6	----	.2	---	----	----	----	-----	---	----	------
Iron base													
19-9DL	64.8	20.4	10	----	1	1.6	----	----	0.3	0.2	---	1.4	0.3Ti
304	68.5	19.8	8.6	----	1.3	1.6	----	----	----	-----	---	.2	------
310	49.4	27.4	19.1	----	1.2	1.4	----	----	----	-----	---	1.1	.5Ti
316	62.2	20.	13.5	----	1.4	1.	1.5	----	----	-----	---	.4	------
347	65.3	21.4	10.5	----	1.	1.4	----	.1	----	-----	---	.4	------
A286 (cw 50 percent)	53.	17.1	22.5	----	1.	1.6	.6	----	----	-----	.4	.4	3.1Ti
Armco 18SR[a]	72.	19.1	1.8	----	.1	2.7	----	----	----	-----	3.6	.2	.6Ti
Inconel 800	45.1	22.6	29.8	----	.6	1.	----	----	----	-----	---	.5	.4Cu
Mild steel	98.6	----	----	----	.5	---	----	----	----	-----	---	.9	------
N-155	31.5	25.1	18.7	18.6	1.	1.6	1.8	.5	----	-----	---	.7	.60N
Nitronic 40	59.3	23.1	7.4	----	7.1	1.7	----	----	----	-----	---	.4	1.2N
PH14-8Mo	70.7	16.4	8.3	----	----	---	.6	1.3	----	-----	2.5	.2	------
RA 330	43.8	21.9	30.	----	1.4	2.5	----	----	----	-----	---	.4	------
Refractory metal													
Mo	----	----	----	----	----	---	99.8	----	----	-----	---	0.2	------
Nb-1Zr	----	----	----	----	----	---	----	98.9	----	-----	---	----	1.1Zr
Ta	----	----	----	----	----	---	----	.2	99.5	-----	---	.15	.13N
W	----	----	----	----	----	---	----	----	----	99.85	---	.15	------

[a]Ferritic alloy; all other iron base alloys are austenitic.

TABLE VIII. - SUMMARY OF ATTACK OF VARIOUS ALLOYS CAUSED BY EXPOSURE TO EUTECTIC FLUORIDE SALT MIXTURES IN ALUMINA CRUCIBLES UNDER 1 atm OF ARGON

Composition, at % Melting point, K Exposure conditions	LiF-19.5CaF_2 1039 100 hr - 1070 K		LiF-19.5CaF_2 1039 500 hr - 1070 K		NaF-27CaF_2-36MgF_2 1178 100 hr - 1203 K	
Alloy	Depth of corrosive attack, μm					
	General	Grain boundary	General	Grain boundary	General	Grain boundary
Co-base						
H-25	--	12	--	95	--	8
	--	--	--	70	--	[a]25
HS-188	--	47	--	105	--	18
Fe-base						
19-9DL	--	--	--	---	--	13
304	--	20	--	185	--	[b]5
310	17	--	--	130	--	5
	--	--	--	---	--	[a]10
316	--	45	--	165	--	10
	--	--	--	---	--	[a]15
347	--	--	--	---	--	[b]8
A286	43	--	--	---	--	10
Armco 18SR	--	--	--	---	--	38
Incoloy 800	--	45	--	---	30	--
Mild steel	--	--	--	155	12	--
	--	--	--	---	--	[a]--
PH14-8	14	--	--	---	10	--
RA-330	--	--	--	270	--	20
Ni-base						
Hastelloy B	8	--	30	---	--	--
	--	--	20	---	--	--
Hastelloy N	--	20	15	15	--	15
	--	--	--	---	--	[a]25
False N	--	27	--	135	--	--
Hastelloy S	--	--	90	---	0	10
Hastelloy X	--	45	--	140	--	[b]38
Inconel 600	13	34	90	30	--	13
Inconel 702	15	60	--	---	--	--
Inconel 718	13	24	45	120	--	8
	--	--	--	---	--	[a]50
Ni-200	--	--	--	---	8	--
	--	--	--	---	18	--
Nimonic 75	--	--	30	135	--	--
Refractory						
Mo	--	--	--	---	--	--
Nb-1Zr	--	--	--	---	--	--
Ta	--	--	--	---	60	--
	--	--	--	---	25	[a]--
W	--	--	--	---	--	--

[a]Exposures conducted with a piece of quartz in the crucible.
[b]No difference between exposures with/without quartz in crucible.

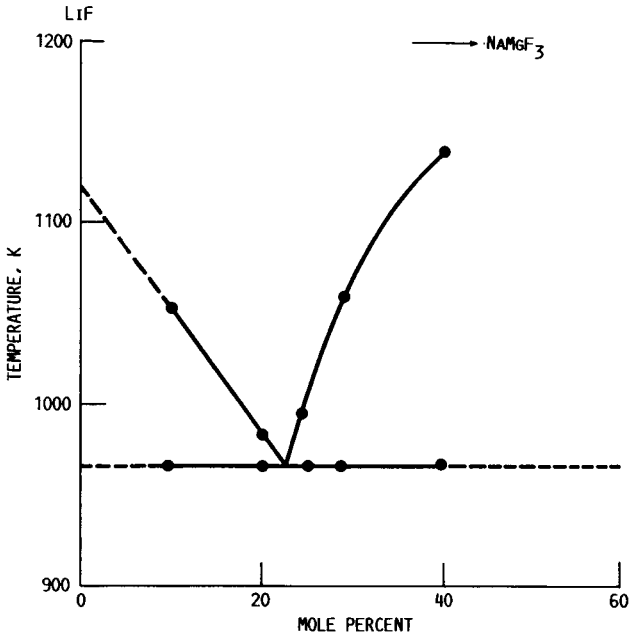

FIGURE 1. - PARTIAL PHASE DIAGRAM FOR THE LiF-$NaMgF_3$ SYSTEM.

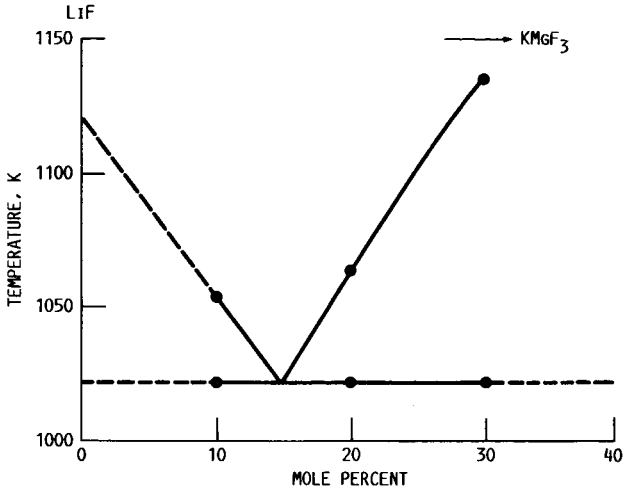

FIGURE 2. - PARTIAL PHASE DIAGRAM FOR THE LiF-$KMgF_3$ SYSTEM.

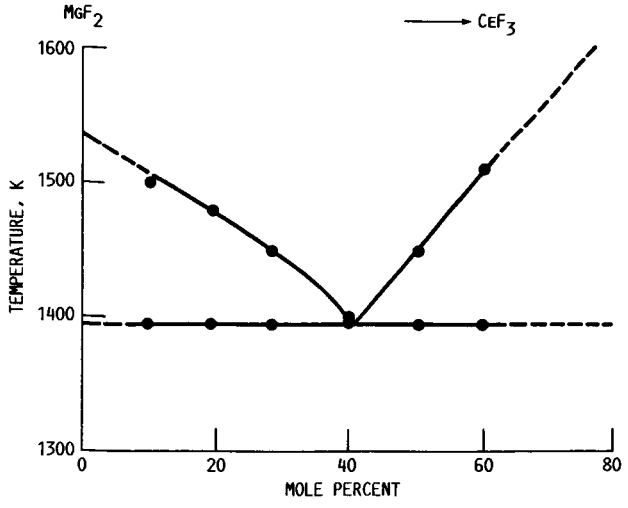

FIGURE 3. - PARTIAL PHASE DIAGRAM FOR THE MgF_2-CeF_3 SYSTEM.

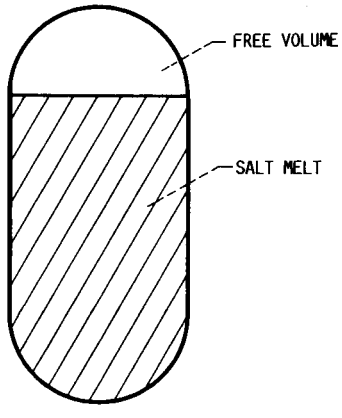

FIGURE 4. - SCHEMATIC OF A THERMAL ENERGY STORAGE SALT CONTAINER.

what makes this report different from the Olson one is that they differentiate between different salts and they have not considered F2. But they had no oxygen, so they are using the same reaction as we are using, but not including the oxygen and the metal oxide. instead of our metal oxide, they have only alkali metal reduced, which makes it quite odd. You are separating a lower potential element, by a more cathodic element like Ni or Cr (compared to the very active Na or Li)

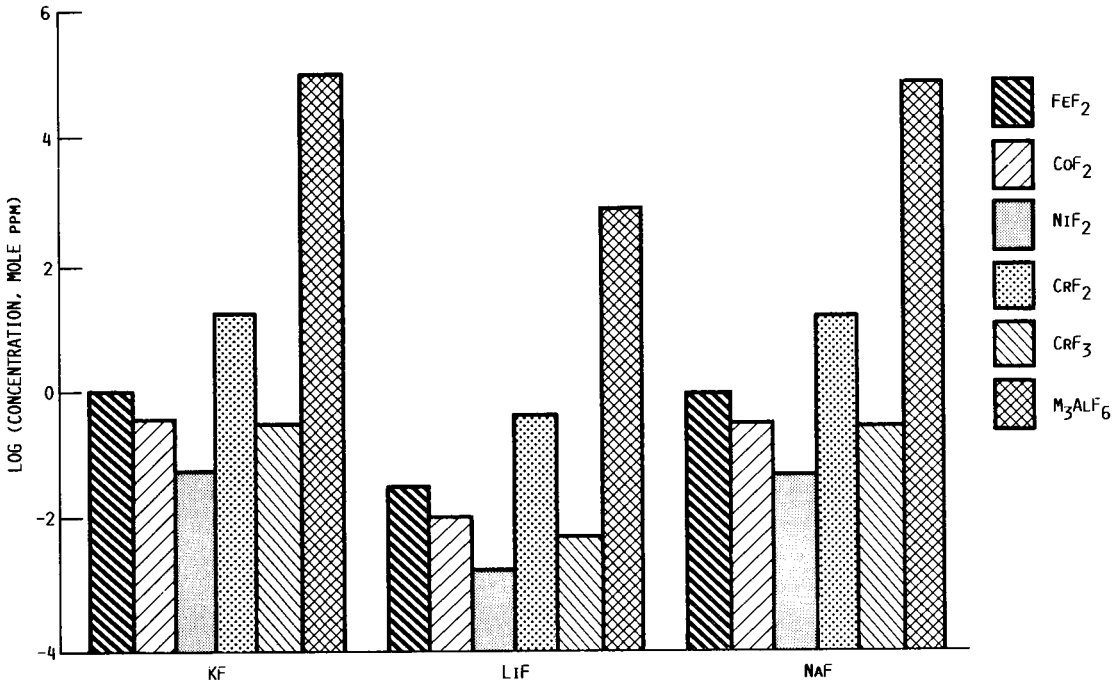

FIGURE 5. - CALCULATED EQUILIBRIUM CONCENTRATION OF Me_xF_y (M = Fe, Ni, Co, Cr, OR Al) AFTER CORROSION IN ONE MOLE OF ALKALI FLUORIDE MELT AT 1100 K IN AN INERT ATMOSPHERE (IDEAL SOLUTION BEHAVIOR IN THE MELT ASSUMED).

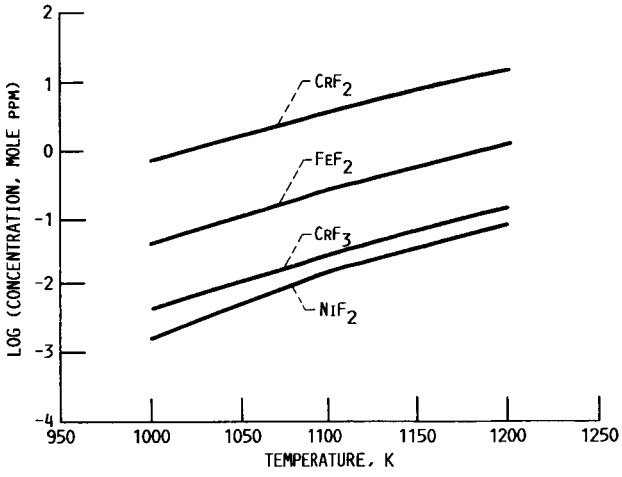

FIGURE 6. - EQUILIBRIUM CONCENTRATION OF Me_xF_y, CALCULATED WITH AN ACTIVITY COEFFICIENT OF 0.001, AFTER CORROSION IN ONE MOLE OF LiF MELT UNDER AN INERT ATMOSPHERE.

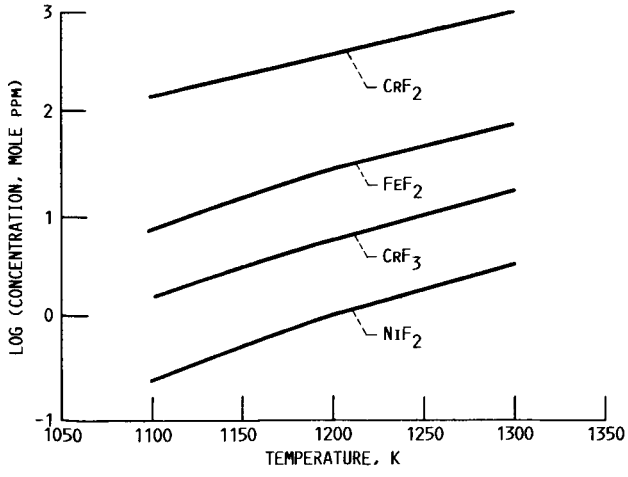

FIGURE 7. - EQUILIBRIUM CONCENTRATION OF Me_xF_y, CALCULATED WITH ESTIMATED ACTIVITY COEFFICIENTS, AFTER CORROSION IN ONE MOLE OF NaF MELT UNDER AN INERT ATMOSPHERE.

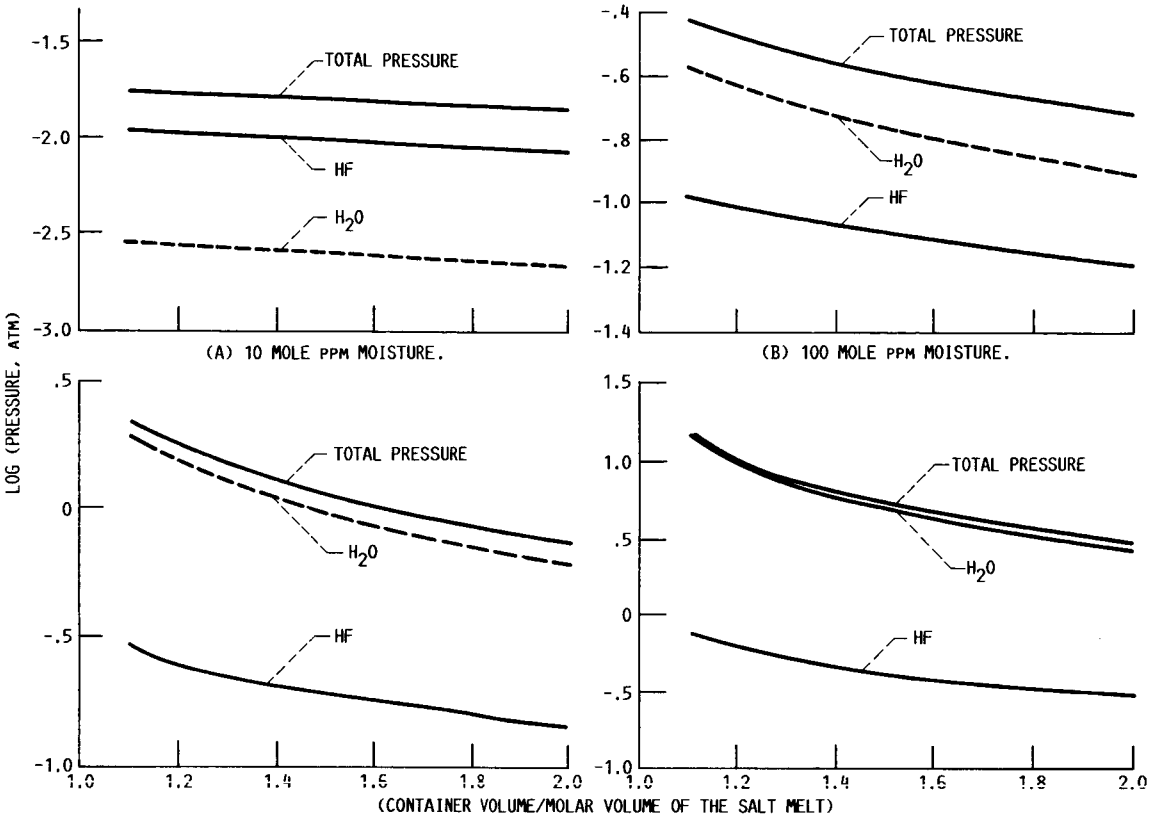

FIGURE 8. - PARTIAL PRESSURES OF HF AND H_2O AND TOTAL PRESSURE INSIDE THE CONTAINER FOR A NaF MELT AT 1100 K AS A FUNCTION OF MOISTURE CONTENT AND L RATIO.

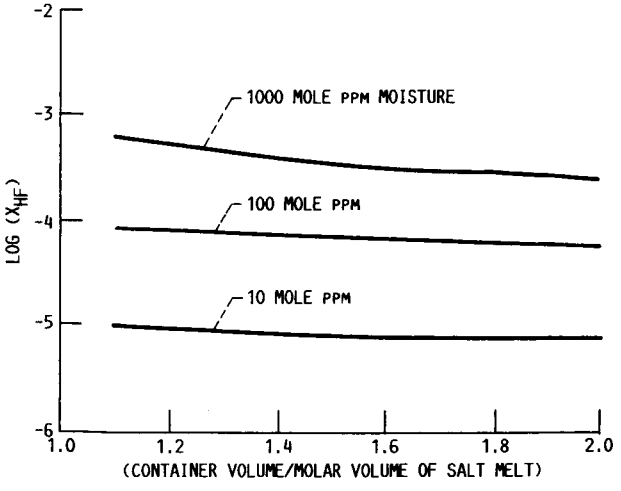

FIGURE 9. - MOLE FRACTION OF DISSOLVED HF (X_{HF}) IN THE MELT AS A FUNCTION OF MOISTURE FOR A NaF MELT AT 1100 K.

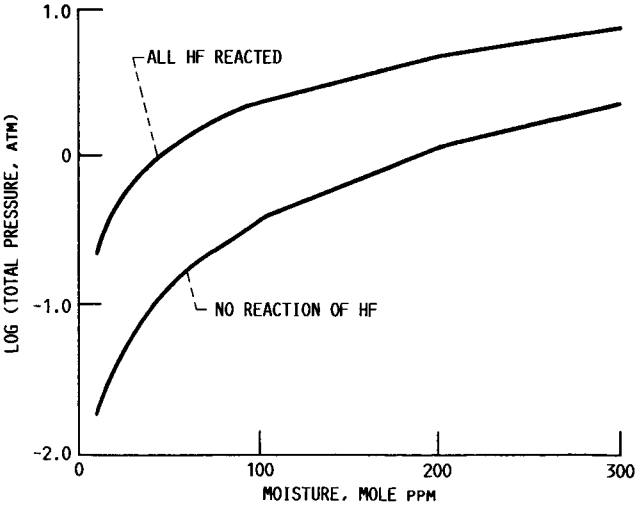

FIGURE 10. - EFFECT OF THE REACTION OF DISSOLVED HF WITH THE CONTAINER MATERIAL ON THE TOTAL PRESSURE GENERATED INSIDE THE CONTAINER.

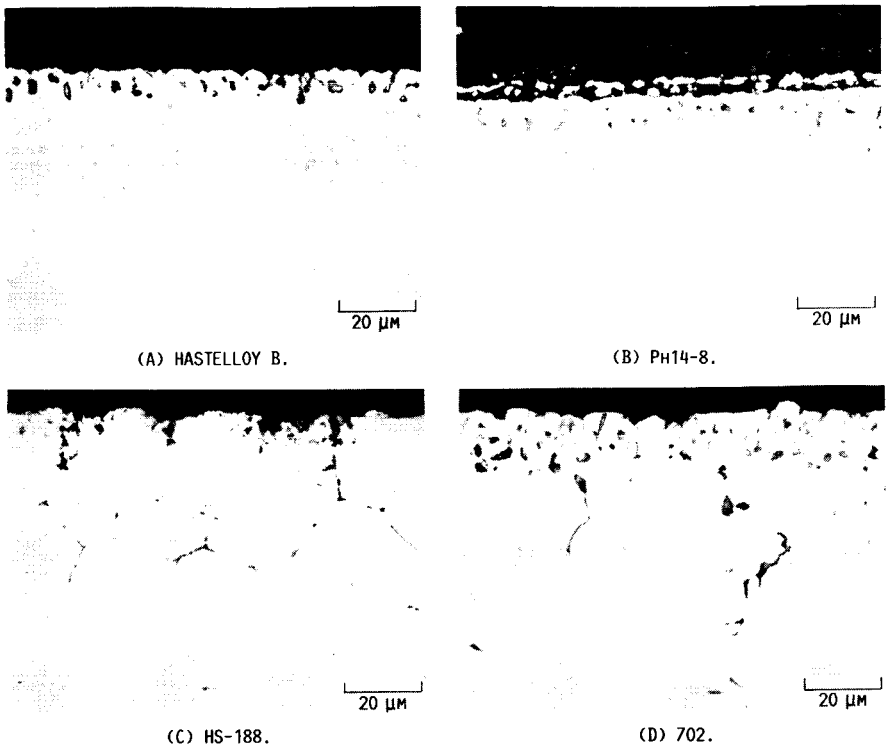

(A) HASTELLOY B. (B) PH14-8.

(C) HS-188. (D) 702.

FIGURE 11. - PHOTOMICROGRAPHS OF SPECIMENS AFTER 100 HR EXPOSURES TO LiF-19.5CaF_2 AT 1070 K IN ALUMINA CRUCIBLES UNDER 1 ATMOSPHERE OF ARGON.

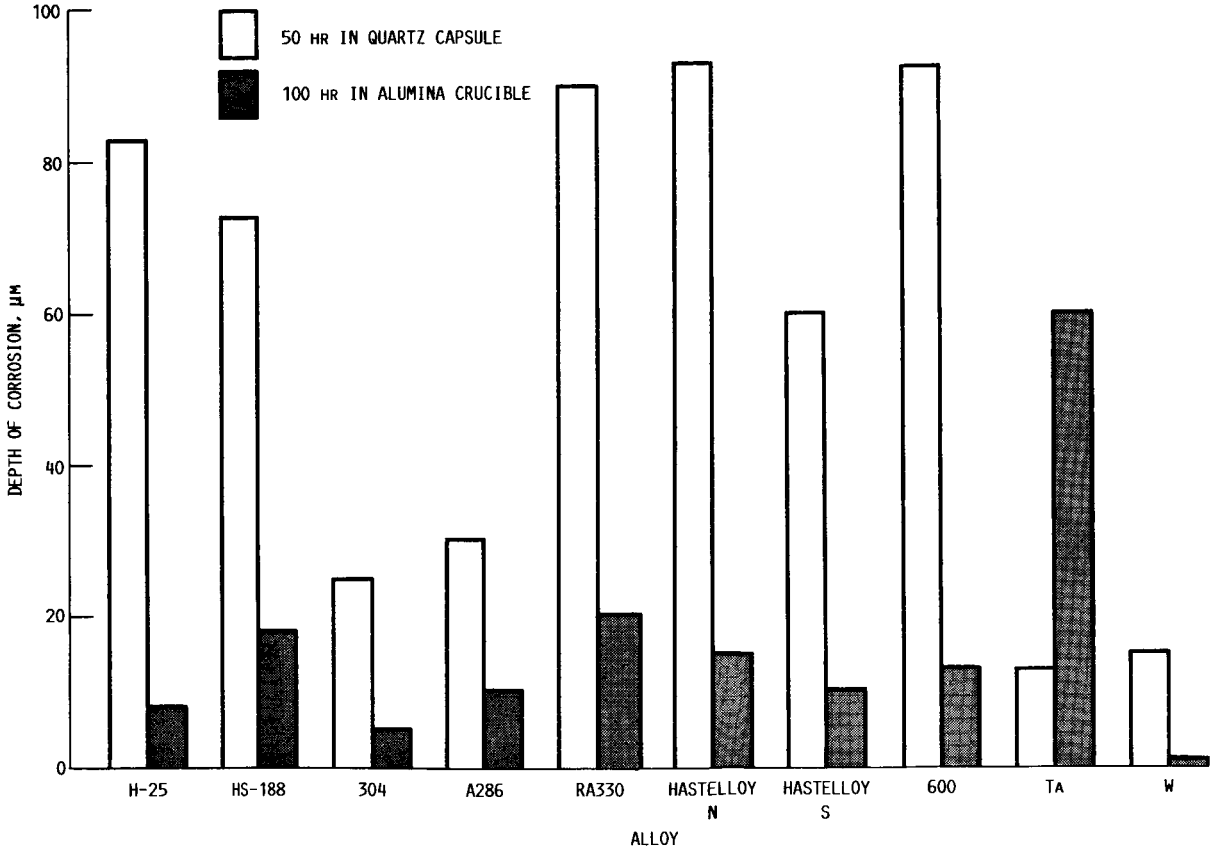

FIGURE 12. - COMPARISON OF THE DEPTH OF CORROSION IN SEVERAL HIGH TEMPERATURE ALLOYS AFTER EXPOSURE TO NaF-27CaF_2-36MgF_2 AT 1203 K IN QUARTZ CAPSULES AND ALUMINA CRUCIBLES.

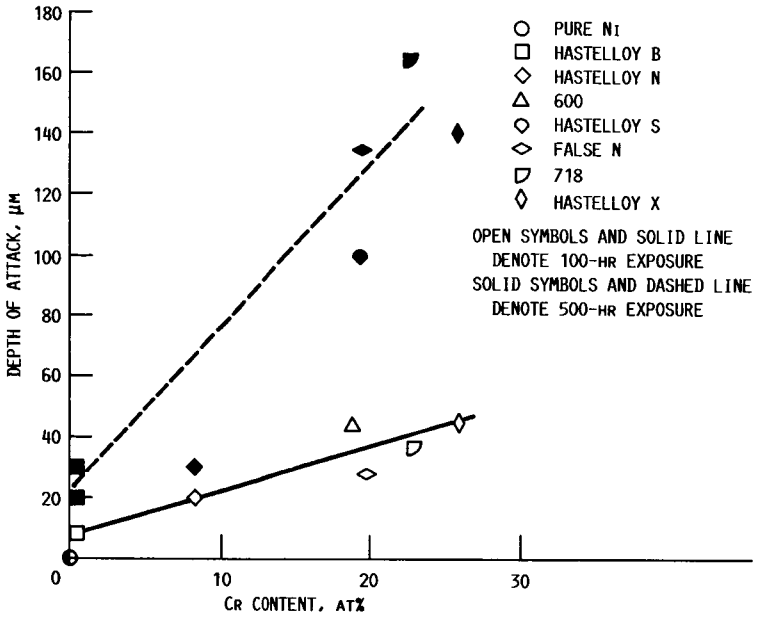

FIGURE 13. - DEPTH OF MICROSTRUCTURAL DAMAGE AS A FUNCTION OF Cr LEVEL FOR ALLOYS EXPOSED TO LiF-19.5CaF_2 AT 1070 K IN ALUMINA CRUCIBLES UNDER 1 ATMOSPHERE OF ARGON.

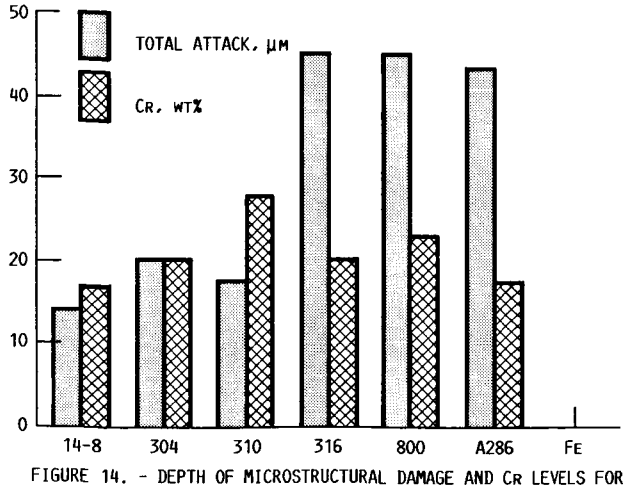

FIGURE 14. - DEPTH OF MICROSTRUCTURAL DAMAGE AND Cr LEVELS FOR Fe-BASE ALLOYS EXPOSED TO LiF-19.5CaF_2 AT 1070 K IN ALUMINA CRUCIBLES UNDER 1 ATMOSPHERE OF ARGON.

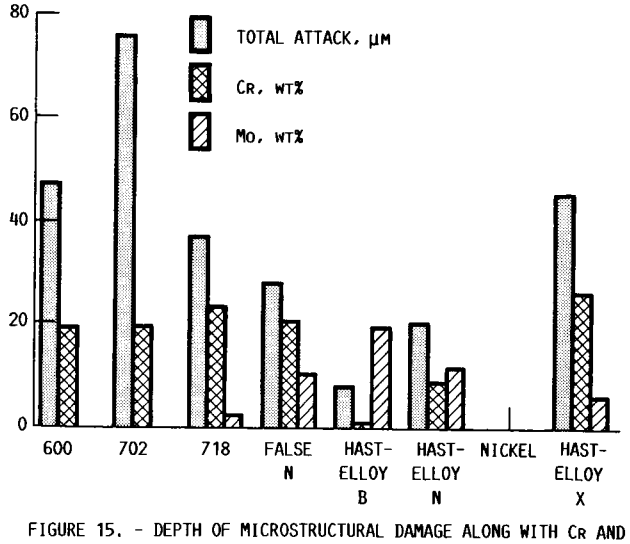

FIGURE 15. - DEPTH OF MICROSTRUCTURAL DAMAGE ALONG WITH Cr AND Mo LEVELS FOR Ni-BASE ALLOYS EXPOSED TO LiF-19.5CaF_2 AT 1070 K IN ALUMINA CRUCIBLES UNDER 1 ATMOSPHERE OF ARGON.

1. Report No.	2. Government Accession No.	3. Recipient's Catalog No.
NASA TM-89913 AIAA-87-9226		

4. Title and Subtitle	5. Report Date
Fluoride Salts and Container Materials for Thermal Energy Storage Applications in the Temperature Range 973 to 1400 K	6. Performing Organization Code 506-41-3A
7. Author(s) Ajay K. Misra and J. Daniel Whittenberger	8. Performing Organization Report No. E-3563
	10. Work Unit No.
9. Performing Organization Name and Address National Aeronautics and Space Administration Lewis Research Center Cleveland, Ohio 44135	11. Contract or Grant No.
	13. Type of Report and Period Covered Technical Memorandum
12. Sponsoring Agency Name and Address National Aeronautics and Space Administration Washington, D.C. 20546	14. Sponsoring Agency Code

15. Supplementary Notes

Prepared for the 22nd Intersociety Energy Conversion Engineering Conference, cosponsored by the AIAA, ANS, ASME, SAE, IEEE, ACS, and AIChE, Philadelphia, Pennsylvania, August 10-14, 1987. Ajay K. Misra, Department of Metallurgy and Materials Science, Case Western Reserve University, Cleveland, Ohio 44106 and NASA Lewis Resident Research Associate.

16. Abstract

Multicomponent fluoride salt mixtures were characterized for use as latent heat of fusion heat storage materials in advanced solar dynamic space power systems with operating temperatures in the range of 973 to 1400 K. The melting points and eutectic compositions for many systems with published phase diagrams were verified, and several new eutectic compositions were identified. Additionally the heats of fusion of several binary and ternary eutectics and congruently melting intermediate compounds were measured by differential scanning calorimetry. The extent of corrosion of various metals by fluoride melts was estimated from thermodynamic considerations, and equilibrium conditions inside a containment vessel were calculated as functions of the initial moisture content of the salt and free volume above the molten salt. Preliminary experimental data on the corrosion of commercial, high-temperature alloys in $LiF-19.5CaF_2$ and $NaF-27CaF_2-36MgF_2$ melts are presented and compared to the thermodynamic predictions.

17. Key Words (Suggested by Author(s))	18. Distribution Statement
Thermal energy storage; Space power; Fluoride salts; Thermodynamics; Corrosion	Unclassified - unlimited STAR Category 44

19. Security Classif. (of this report)	20. Security Classif. (of this page)	21. No. of pages	22. Price*
Unclassified	Unclassified	22	A02

*For sale by the National Technical Information Service, Springfield, Virginia 22161